

The Interaction in the Macroscopically Ordered Exciton State

Sen Yang, A.V. Mintsev,* A.T. Hammack, and L.V. Butov

Department of Physics, University of California at San Diego, La Jolla, CA 92093-0319

A.C. Gossard

Materials Department, University of California at Santa Barbara, Santa Barbara, CA 93106-5050

(Dated: March 23, 2022)

The macroscopically ordered exciton state (MOES) - a periodic array of beads with spatial order on a macroscopic length - appears in the external exciton rings at low temperatures below a few Kelvin. Here, we report on the experimental study of the interaction in the MOES. The exciton PL energy varies in concert with the intensity along the circumference of the ring, with the largest energy found in the brightest regions. This shows that the MOES is characterized by the repulsive interaction and is not driven by the attractive interaction.

Spatial photoluminescence (PL) patterns have been observed recently in structures with coupled^{1,2,3} and single⁴ quantum wells. The pattern features include the inner exciton rings¹, the external exciton rings^{1,2,3,4}, the localized bright spots (LBS)^{1,3,5,6}, and the macroscopically ordered exciton state (MOES) - a periodic array of beads with spatial order on a macroscopic length^{1,3}. The inner and outer exciton rings and LBS are observed up to high temperatures and are classical phenomena. Their origin has been identified: the inner ring has been explained in terms of nonradiative exciton transport and cooling⁷ and the external rings and LBS have been explained in terms of macroscopic in-plane charge separation and exciton formation at the interface of the electron- and hole-rich regions^{3,4}. On the contrary, the MOES is a low-temperature phenomenon. The MOES appears in the external rings at low temperatures below a few Kelvin^{1,3}. Because of their long lifetime and high cooling rate, indirect excitons in coupled quantum wells (CQW), Fig. 1a, form a system where a cold and dense exciton gas can be created⁸. Research to understand the origin of the MOES is in progress.

Spontaneous macroscopic ordering is a general phenomenon in pattern formation. For instance, the MOES is characterized by a 1D spatial modulation and periodic 1D patterns are observed in a variety of both quantum and classical systems. The examples include the soliton trains in atom Bose-Einstein condensates (BEC)⁹, Taylor vortices in liquids¹⁰, Turing instabilities in reaction-diffusion systems¹¹ and bacteria colonies¹², and gravitational instabilities in cosmological systems¹³. All of these ordered states originate from an instability, which is generated by a positive feedback to density modulation. A particular mechanism of the positive feedback, which is responsible for the soliton train formation⁹ and gravitational instability¹³, is an attractive interaction: In the experiments on atom BEC, the stripe of atomic BEC was homogeneous in the case of repulsive interaction and, conversely, was fragmented to the periodic soliton train in the case of attractive interaction due to the modulational instability⁹; Gravitational instability results in the fragmentation of gaseous slabs and filaments to a periodic array of high-density clumps that is a step towards

the formation of stars¹³.

In this paper, we address an issue of interaction in MOES. An attractive interaction could in principle lead to the density modulation in the exciton ring, i.e. to the MOES formation. However, our experimental results indicate that the interaction is repulsive in MOES. Therefore, the interaction cannot be responsible for the MOES formation and, on the contrary, acts against the density modulation.

An electric-field-tunable $n^+ - i - n^+$ GaAs/(Al,Ga)As CQW structure was grown by molecular beam epitaxy. The i -region consists of two 8 nm GaAs QWs separated by 4 nm $\text{Al}_{0.33}\text{Ga}_{0.67}\text{As}$ barrier and surrounded by two 200 nm $\text{Al}_{0.33}\text{Ga}_{0.67}\text{As}$ barrier layers. The n^+ -layers are Si-doped GaAs with $N_{\text{Si}} = 5 \times 10^{17} \text{ cm}^{-3}$. The electric field in the z -direction is created by the external gate voltage V_g applied between n^+ -layers. Details on the CQW structures can be found in Ref.⁸. The indirect excitons in the CQW structure are formed from electrons and holes confined to different QWs (Fig. 1a). The carriers were excited by cw HeNe laser. The small disorder in the CQW is indicated by the PL linewidth of about 1 meV. The experiments were performed in a He⁴ optical cryostat.

The spatial $x - y$ photoluminescence (PL) pattern was measured by a liquid-nitrogen-cooled CCD camera after spectral selection by an $800 \pm 5 \text{ nm}$ interference filter chosen to match the indirect exciton energy. As a result, the low-energy bulk emission, higher-energy direct exciton emission, and scattered laser light were effectively removed and the indirect exciton PL emission intensity was directly visualized in $x - y$ spatial coordinates. The scheme of the experiment is shown in Fig. 1b. Fig. 1d shows the indirect exciton PL pattern at $T = 1.6 \text{ K}$ and excitation power $P_{\text{ex}} = 0.25 \text{ mW}$. The laser excitation spot is in the center of the image. The external exciton ring, LBS, and MOES are clearly seen in the image (the inner exciton ring is not seen for the presented contrast and its images can be found in Ref.⁷).

In addition, we measured the exciton PL energy profiles along the ring using the experimental scheme shown in Fig. 1c: a segment of the ring was projected on the spectrometer slit and the image was dispersed by a spec-

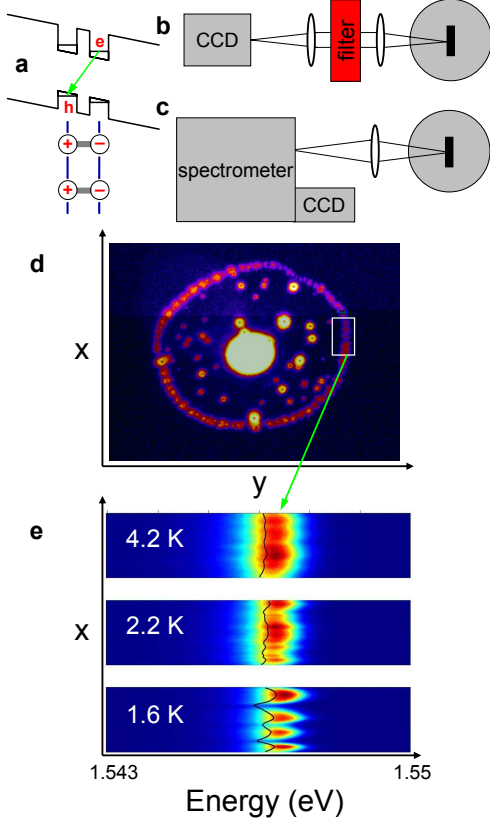


FIG. 1: (a) Energy band diagram of the CQW structure; e is electron, h - hole. (b) Scheme of the experimental setup for imaging PL signals in $x - y$ coordinates (b) and $E - x$ coordinates (c). (d) PL image of indirect excitons in $x - y$ coordinates at $T = 1.6$ K. The area of view is $365 \times 275 \mu\text{m}$. (e) Spectrally resolved PL image of indirect excitons in $E - x$ coordinates for the ring segment, which is marked by a rectangle in (d), at $T = 1.6, 2.2$, and 4.2 K. The length of view (vertical axis) is $50 \mu\text{m}$ for each image. The black lines show variation of the PL energy of the indirect excitons along the circumference of the ring. $V_g = 1.211$ V and $P_{ex} = 0.25$ mW for the data.

trometer without spectral selection by an interference filter. The selected part of the external ring was parallel to the spectrometer entrance slit and the slit width (0.1mm) was small enough to get a high spectral resolution (0.1nm) and spatial resolution in the x -direction ($2\mu\text{m}$). The measured images of the PL signal in the *energy-coordinate* plane are presented in Fig. 1e for different temperatures.

Fig. 1e shows the indirect exciton energy profile along the selected part of the ring. The black lines show variation of the average PL energy $E_{PL}(x) = \frac{\int \int E(x, y, \lambda) I(x, y, \lambda) dy d\lambda}{\int \int I(x, y, \lambda) dy d\lambda}$ of the indirect excitons along the circumference of the ring. The indirect exciton PL intensity modulation increases drastically with reducing temperature, which indicates formation of the MOES. This is consistent with the earlier studies^{1,3}. The measure-

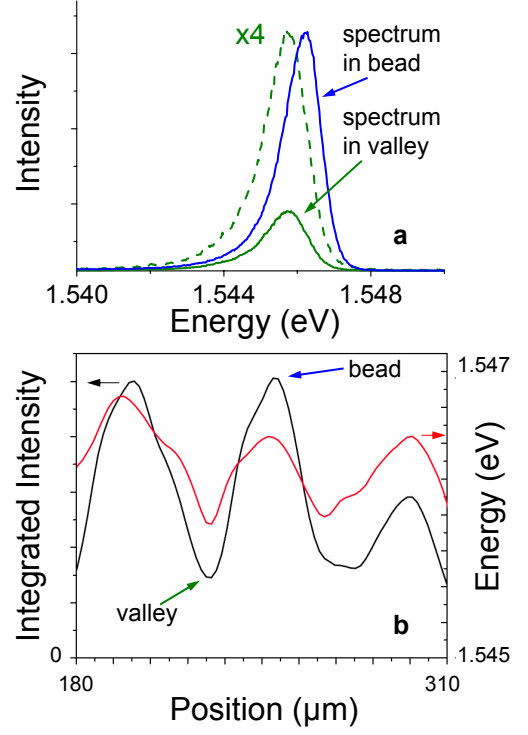


FIG. 2: (a) The indirect exciton PL spectrum in the bead center (bold blue line) and in between two beads (thin green line, dashed green line shows the same spectrum multiplied by a factor of 4 for comparison). (b) Variation of the PL energy and intensity of the indirect excitons along the circumference of the ring. $T = 1.6$ K, $V_g = 1.30$ V and $P_{ex} = 8.6\text{mW}$ for the data. The indirect exciton energy increases with increasing density indicating repulsive interaction in the regime of MOES.

ments presented in Fig. 1e show that the increase of PL intensity modulation with reducing temperature is accompanied by the increase of PL energy modulation.

The variations of the spectrally integrated PL intensity $I_{PL}(x) = \int \int I(x, y, \lambda) dy d\lambda$ and average energy $E_{PL}(x)$ of the indirect excitons along the circumference of the ring are shown in Fig. 2b. The PL energy varies in concert with the intensity along the circumference of the ring, with the largest energy found in the brightest regions. The corresponding spectra in a bead center and in a valley between two beads are shown on Fig. 2a. The indirect exciton PL intensity and energy are higher in the bead center.

The CQW geometry⁸ is engineered so that the interaction between excitons is repulsive: Indirect excitons, formed from electrons and holes confined to different QWs, behave as dipoles oriented perpendicular to the plane and an exciton or electron-hole density increase causes an enhancement of energy^{14,15,16}. The repulsive character of interaction was evident in earlier experiments as a positive line shift with increasing density¹⁷. Observation of the same behavior in the regime of the

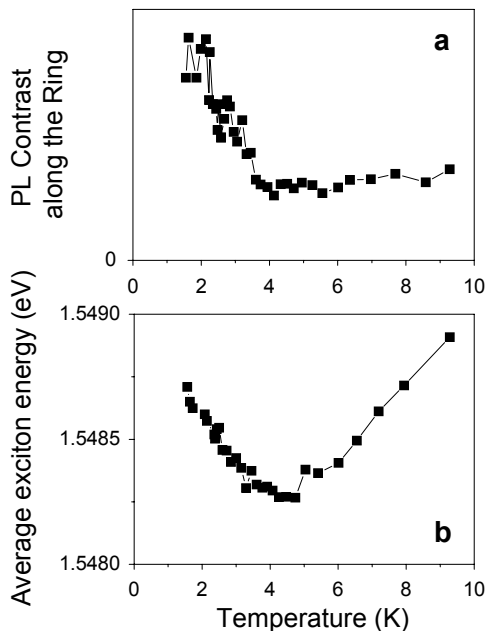


FIG. 3: (a) Exciton density Fourier transform peak height at the fragmentation period and (b) spatially averaged energy of indirect excitons in the ring vs. temperature. $V_g = 1.15V$ and $P_{ex} = 118\mu W$ for the data.

MOES (Fig. 2) shows that the MOES is characterized by the repulsive interaction and is not driven by the attractive interaction.

We have also addressed an issue whether formation of MOES lowers the total energy of the exciton system in the ring. For this purpose, we measured the spatially average energy of indirect excitons in the external ring

$E_{avg} = \frac{\int \int \int E(x,y,\lambda) I(x,y,\lambda) dx dy d\lambda}{\int \int \int I(x,y,\lambda) dx dy d\lambda}$ as a function of temperature, see Fig. 3b. Exciton density Fourier transform peak height at the fragmentation period, which characterized the density modulation contrast, is also presented in Fig. 3a for comparison. Fig. 3b shows that the average energy of the indirect excitons in the ring depends non monotonically on temperature with a transition around $T_{tr} \sim 4$ K: with reducing temperature, the energy reduces above T_{tr} and increases below T_{tr} . Note that the average indirect exciton PL energy exhibits a transition simultaneously with the MOES onset at ca. 4 K, compare Fig. 3a and Fig. 3b.

Fig. 3 indicates that MOES formation is accompanied by an increase of the total energy of excitons in the ring and, therefore, the density modulation is not caused by lowering the total energy of the system. Note that such a behavior is not unusual for pattern formations in quasi-equilibrium systems and, in particular, is consistent with a model¹⁸ showing that a spatially modulated exciton state can result from a nonlinear density dependence of the exciton formation rate in the ring.

To conclude, the exciton PL energy has been found to vary in concert with the intensity along the circumference of the ring for the macroscopically ordered exciton state. This shows that MOES is characterized by the repulsive interaction and eliminates attractive interaction as a possible mechanism that could lead to the MOES formation.

This work is supported by NSF grant DMR-0606543 and ARO grant W911NF-05-1-0527. We thank K.L. Campman for growing the high quality samples, J. Keeling, L.S. Levitov, and B.D. Simons for discussions, G.O. Andreev and E. Shipton for help in preparing the experiment.

* Present address: Institute of Solid State Physics, Russian Academy of Sciences, 142432 Chernogolovka, Russia

¹ L.V. Butov, A.C. Gossard, and D.S. Chemla, cond-mat/0204482; Nature **418**, 751 (2002).

² D. Snoke, S. Denev, Y. Liu, L. Pfeiffer, and K. West, Nature **418**, 754 (2002).

³ L.V. Butov, L.S. Levitov, A.V. Mintsev, B.D. Simons, A.C. Gossard, and D.S. Chemla, cond-mat/0308117; Phys. Rev. Lett. **92**, 117404 (2004).

⁴ R. Rapaport, G. Chen, D. Snoke, S.H. Simon, L. Pfeiffer, K. West, Y. Liu, and S. Denev, cond-mat/0308150; Phys. Rev. Lett. **92**, 117405 (2004).

⁵ L.V. Butov, C.W. Lai, A.L. Ivanov, A.C. Gossard, and D.S. Chemla, Nature **417**, 47 (2002).

⁶ C.W. Lai, J. Zoch, A.C. Gossard, and D.S. Chemla, Science **303**, 503 (2004).

⁷ A.L. Ivanov, L.E. Smallwood, A.T. Hammack, Sen Yang, L.V. Butov, and A.C. Gossard, Europhys. Lett. **73**, 920 (2006).

⁸ L.V. Butov, J. Phys.: Condens. Matter **16**, R1577 (2004).

⁹ K.E. Strecker, G.B. Partridge, A.G. Truscott, and R.G. Hulet, Nature **417**, 150 (2002).

¹⁰ G.I. Taylor, Phil. Trans. R. Soc. A **223**, 289 (1923).

¹¹ V. Castets, E. Dulos, J. Boissonade, and P. De Kepper, Phys. Rev. Lett. **64**, 2953 (1990).

¹² E.B. Jacob, I. Becker, Y. Shapira, and H. Levine, Trends in Microbiology **12**, 366 (2004).

¹³ S. Chandrasekhar and E. Fermi, Astrophys. J. **118**, 116 (1953).

¹⁴ D. Yoshioka and A.H. MacDonald, J. Phys. Soc. Jpn. **59**, 4211 (1990).

¹⁵ X. Zhu, P.B. Littlewood, M. Hybertsen, and T.M. Rice, Phys. Rev. Lett. **74**, 1633 (1995).

¹⁶ Yu.E. Lozovik and O.L. Berman, JETP Lett. **64**, 573 (1996).

¹⁷ L. V. Butov, A. Zrenner, G. Abstreiter, G. Böhm, and G. Weimann, Phys. Rev. Lett. **73**, 304 (1994).

¹⁸ L.S. Levitov, B.D. Simons, and L.V. Butov, Phys. Rev. Lett. **94**, 176404 (2005).